Colloid Polym Sci (2009) 287:839–846
DOI 10.1007/s00396-009-2038-8

ORIGINAL CONTRIBUTION

Strong effect of NaBr on self-assembly of quaternary ammonium gemini surfactants at air/water interface and in aqueous solution studied by surface tension and fluorescence techniques

Yi You · Jianxi Zhao · Rong Jiang · Jingjing Cao

Received: 13 January 2009 / Revised: 20 March 2009 / Accepted: 2 April 2009 / Published online: 29 April 2009

Abstract The effects of NaBr on the adsorption of alkanediyl-bis-(dimethyl dodecyl- ammonium bromide) (referred to as C_{12}-*s*-C_{12} 2Br) at the air/water interface and on the micellization in the solution have been investigated by surface tension and fluorescence techniques. The results showed that the addition of NaBr greatly enhances their efficiency and effectiveness in surface tension reduction as well as the ability of micellization, even induces strong premicellar aggregation before the *cmc*. These were attributed to the unique molecular structure of gemini surfactant, where the flexible polymethylene chain was the spacer linking the two quaternary ammonium heads. By a short spacer, the charges of the two quaternary ammonium head groups are concentrated. Even for a long spacer (s=12), since it is bent toward the alkyl tails, the similar effect is also produced. This results in the high sensitivity of their ionic head groups to salt. Besides, the addition of salt also effectively promotes the hydrophobic interaction between the alkyl tails of gemini surfactants.

Keywords Gemini surfactant · Self-assembly · Salt effect

Introduction

It is well known that inorganic salt affects the adsorption of ionic surfactants at air/water interface and the aggregation of them in aqueous solution since the salt screens the charges of ionic head groups and results in the reduction of the electrostatic repulsion between the head groups within the adsorption film and the micelle [1]. Different from conventional surfactants, a molecule of gemini surfactant consists of two hydrophilic head groups, two hydrophobic tails, and a spacer linked at the head groups [2, 3]. The most important characteristic of gemini molecule lies in its "head region" where two ionic head groups are covalently linked by a spacer of variable length [4–7]. This makes the distance between the two ionic head groups controllable by the length of spacer [8]. For example, alkanediyl-bis-(dimethyl alkyl-ammonium bromide), which is referred to as C_m-*s*-C_m 2Br and is a series of typical cationic gemini surfactants investigated extensively [9, 10], has the flexible polymethylene chain as their spacer. The stretched length of the spacer (d_s) can be calculated by the formula d_s/(nm)= 0.127(s+1) [8]. At s=2, d_s is 0.381 nm that is quite smaller than the electrostatic equilibrium distance between the two heads of C_{12}TABr packed on the micelle, which was estimated to be approximately 0.9 nm [8]. This makes the charges of the two head groups of C_m-2-C_m 2Br considerably concentrated and thus it is very sensitive to added salt. Until s=6, d_s (0.889 nm) is just close to the electrostatic equilibrium distance. Further increasing s, Alami et al. [11] confirmed that the flexible polymethylene chain bends toward the alkyl tails at $s \geq 10$–12 for those molecules adsorbed at the air/water interface. As a result, the distance between the two ionic head groups is again decreased and the sensitivity to salt is raised. Thus, it is easily expected that the addition of salt can effectively promote the self-assembly of C_m-*s*-C_m 2Br. In the present paper, we examine the effect of NaBr on the adsorption and the micellization of C_{12}-*s*-C_{12} 2Br in aqueous solution by surface tension and fluorescence techniques. The results indeed show a high sensitivity of the self-assemblies of C_{12}-*s*-C_{12} 2Br to NaBr.

Y. You · J. Zhao (✉) · R. Jiang · J. Cao
Department of Applied Chemistry,
College of Chemistry and Chemical Engineering,
Fuzhou University,
Fuzhou 350002, People's Republic of China
e-mail: jxzhao.colloid@fzu.edu.cn

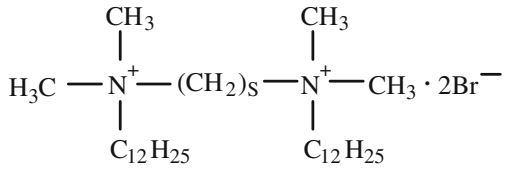

Scheme 1 Molecular structure of C_{12}-*s*-C_{12} 2Br

Experimental

Materials

The molecular structure of alkanediyl-α,ω-bis(dimethyl dodecyl-ammonium bromide) (designated as C_{12}-*s*-C_{12} 2Br, *s*=2, 3, 4, 5, 6, 8) is represented as follows (Scheme 1):

These compounds were synthesized in our laboratory with the method reported by Zana et al. [4], where C_{12}-2-C_{12} 2Br was synthesized by the reaction of *N*,*N*,*N*,'*N*,'-tetramethylethylenediamine with 1-bromo-*n*-dodecane; the other compounds were synthesized by the reaction of *N*,*N*,*N*-dodecyldimethylamine with α,ω-dibromoalkanes. Dodecyltrimethylammonium bromide (C_{12}TABr, Sigma) was recrystallized five times in ethanol–ether mixed solvent. Sodium bromide (NaBr, purity>99%) was purchased from Beijing Chemical Reagents Co. and used as received. Pyrene (Py, Fluka) was recrystallized three times in ethanol. Water used was Milli-Q grade.

Experimental methods

Surface tension of the solutions was measured by du Noüy ring method using tension meter (CHAN DCA-315, America). The circumference of the ring is 5.930 cm. The ratio of the outside radius to the radius of the ring cross section (*R*/*r*) is 53.1218.

Fluorescence emission spectra of pyrene (5×10^{-6}mol L^{-1}) were recorded by Edinburgh FL/FS920 TCSPC fluorescence spectrophotometer (Edinburgh, UK) at an excitation wavelength of 335 nm. Such emission spectra were used to determine the formation of pyrene excimers [12].

All measurements were carried out at 25±0.1°C.

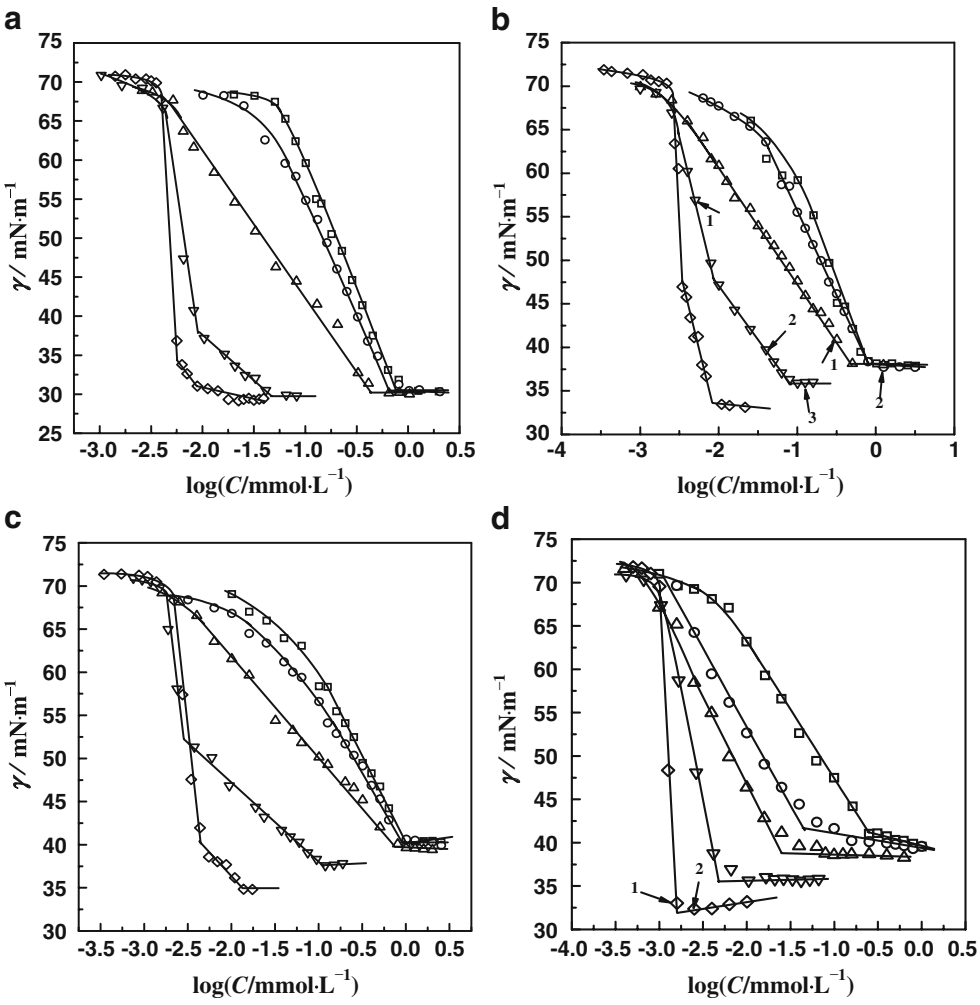

Fig. 1 Semilogarithmic plots of surface tension (γ) as a function of the concentration (*C*) of C_{12}-*s*-C_{12} 2Br at different concentrations of NaBr and at 25°C. **a**, **b**, **c**, and **d** are C_{12}-2-C_{12} 2Br, C_{12}-4-C_{12} 2Br, C_{12}-6-C_{12} 2Br, and C_{12}-12-C_{12} 2Br systems, respectively. The symbols represent: (*squares*) without salt, (*circles*) 0.1 mmol L^{-1}, (*upright triangles*) 1 mmol L^{-1}, (*inverted triangles*) 10 mmol L^{-1}, and (*diamonds*) 100 mmol L^{-1} NaBr

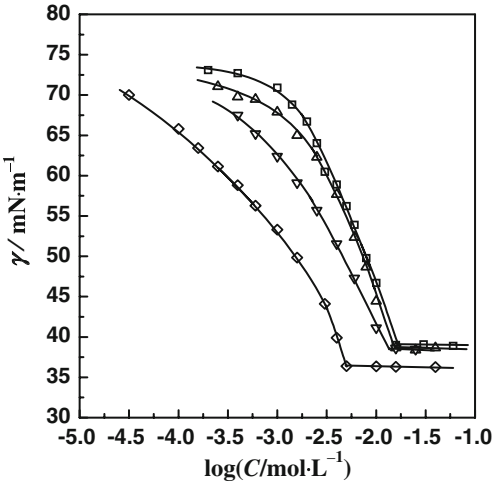

Fig. 2 Semilogarithmic plots of γ as a function of the C of C_{12}TABr at different concentrations of NaBr and at 25°C. The symbols represent: (*squares*) without salt, (*upright triangles*) 1 mmol L^{-1}, (*inverted triangles*) 10 mmol L^{-1}, and (*diamonds*) 100 mmol L^{-1} NaBr

Results and discussion

Surface tension plots

Figure 1 shows the semilogarithmic plots of surface tension (γ) against the concentration (C) of surfactant in aqueous solution in the absence and the presence of NaBr. For comparison, the surface tension plots of C_{12}TABr that is considered as the corresponding monomer of C_{12}-*s*-C_{12} 2Br are shown in Fig. 2. The characteristic parameters obtained from Figs. 1 and 2 are listed in Table 1.

Compared with C_{12}TABr case, Fig. 1 exhibits two important characteristics, i.e., at the relatively high concentration of salt such as 10 and 100 mmol L^{-1}, the rapid drop of surface tension over a very narrow range of the surfactant concentration as well as the two marked break points in the corresponding curve. The rapid drop in γ indicates strong adsorption of C_{12}-*s*-C_{12} 2Br at the interface, and the two break points on the γ versus log$C$ curve generally mean premicellar aggregation in aqueous solution before the saturated adsorption of the surfactant molecules at the air/water interface [13]. They both reflect strong effect of NaBr on the self-assembly of C_{12}-*s*-C_{12} 2Br, which will be discussed in the following sections.

I_1/I_3 plots

The pyrene intensity ratio I_1/I_3 is used as an indication of the polarity of the solubilizing medium for C_{12}-*s*-C_{12} 2Br solutions in the absence and the presence of NaBr (Fig. 3, where the cases without and with 1 and 10 mmol L^{-1} NaBr are taken as the examples). All plots of the I_1/I_3 versus C show a rapid decrease as the surfactant concentration is increased, associated to the formation of aggregates. The

Table 1 The characteristic parameters in the absence and the presence of NaBr

C_{NaBr}/mmol L^{-1}	0	0.1	1	10	100
pC_{20}					
C_{12}-2-C_{12} 2Br	−3.75	−3.90	−4.51	−5.20	−5.33
C_{12}-4-C_{12} 2Br	−3.66	−3.81	−4.36	−5.17	−5.48
C_{12}-6-C_{12} 2Br	−3.58	−3.71	−4.16	−5.51	−5.48
C_{12}-12-C_{12} 2Br	−4.47	−4.96	−5.27	−5.64	−5.92
C_{12}TABr	−2.10	–	−2.13	−2.34	−2.82
γ_{cmc}/mN m^{-1}					
C_{12}-2-C_{12} 2Br	30.6	30.5	30.2	29.8	29.8
C_{12}-4-C_{12} 2Br	38.0	38.0	38.0	35.9	33.5
C_{12}-6-C_{12} 2Br	40.1	40.1	40.0	37.7	35.0
C_{12}-12-C_{12} 2Br	42.5	42.4	38.8	35.6	31.9
C_{12}TABr	39.1	–	38.7	38.6	36.3
cmc/mmol L^{-1}					
C_{12}-2-C_{12} 2Br	0.82 [0.80]	0.65	0.46 [0.43]	0.047 [0.045] (0.0083)	0.013 (0.0057)
C_{12}-4-C_{12} 2Br	0.96 [0.94]	0.76	0.50 [0.69]	0.071 [0.17, 0.074_{mid}] (0.0086)	0.008 (0.0034)
C_{12}-6-C_{12} 2Br	1.01 [1.14]	0.92	0.77 [0.98]	0.10 [0.29, 0.063_{mid}] (0.0030)	0.014 (0.0044)
C_{12}-12-C_{12} 2Br	0.25 [0.32]	0.044	0.025 [0.14, 0.070_{mid}]	0.0050 [0.051, 0.015_{mid}]	0.0020
C_{12}TABr	16.5	–	15.3	13.6	4.82

The data in the square brackets are the *cmc*s measured by pyrene probe method, in which the first and the second values are obtained in terms of procedures 1 and 2, respectively (Fig. 2), and the data in the parentheses are surfactant concentrations at the first break points of surface tension plots

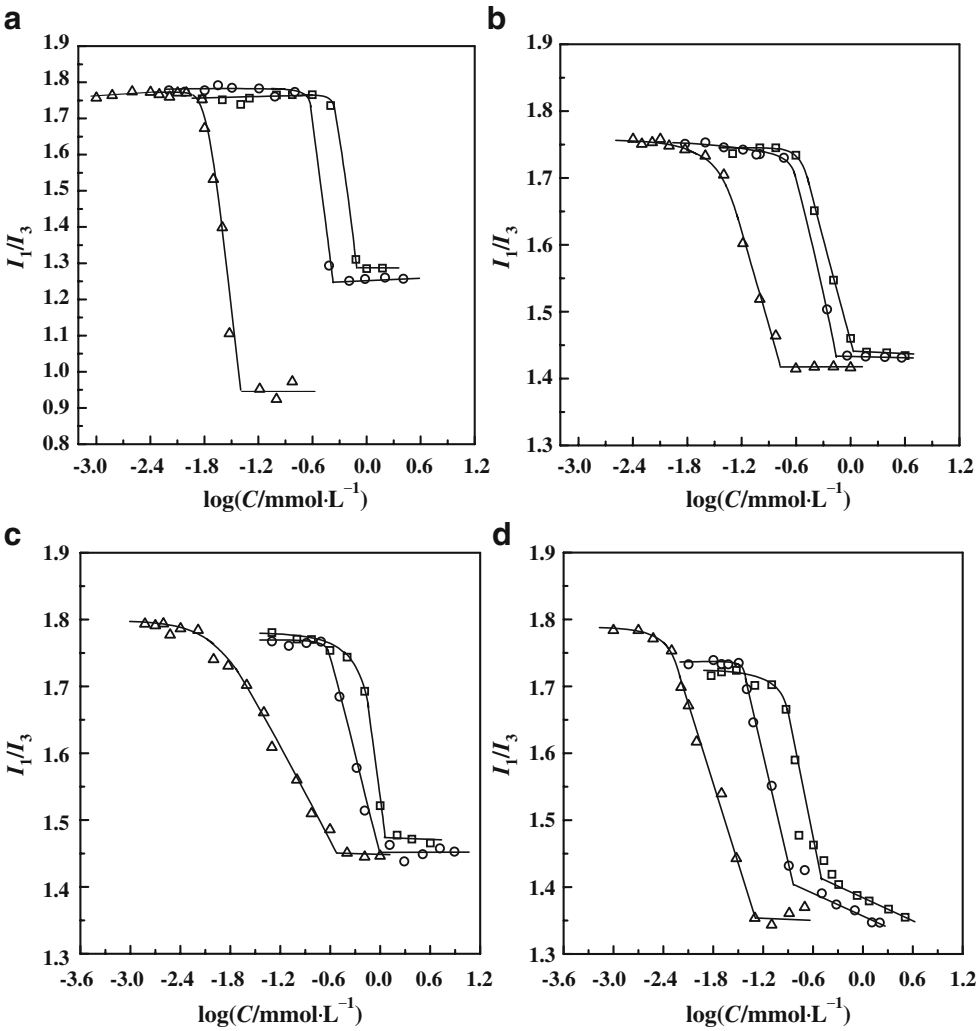

Fig. 3 Variance of the intensity ratio I_1/I_3 for the solutions of C_{12}-2-C_{12} 2Br (**a**), C_{12}-4-C_{12} 2Br (**b**), C_{12}-6-C_{12} 2Br (**c**), and C_{12}-12-C_{12} 2Br (**d**) in the absence (*squares*) and in the presence (*upright triangles*, 1 mmol L^{-1} and *inverted triangles*, 10 mmol L^{-1}) of NaBr with the surfactant concentration at 25°C

cmc is usually taken as the concentration at the intercept of the rapidly varying part and the nearly horizontal part at high concentration of the I_1/I_3 plot (procedure 1) [14, 15]. The *cmc* values yielded by this procedure (see the first values in the square brackets in Table 1) are very close to or slightly larger than that without and with 1 mmol L^{-1} NaBr obtained by surface tension method but evidently larger than that with 10 mmol L^{-1} NaBr. For surfactants with very low *cmc*, Zana et al. [15] also observed that the *cmc* value obtained by the I_1/I_3 plot is larger than that measured by conductivity. This can be explained in terms of pyrene partition between micelles and bulk phase [16]. Since the volume of the hydrophobic core is very small at concentration just above the *cmc*, the pyrene partitions between this phase and the intermicellar solution, thereby reporting an average environment of partly polar character. For this circumstance, Zana et al. [15] suggested that the concentration at mid-decrease of I_1/I_3 (procedure 2) is possibly more suitable for addressing *cmc*. The *cmc*s obtained by procedure 2 are listed in the square brackets as the second values for the cases with 10 mmol L^{-1} NaBr except C_{12}-2-C_{12} 2Br (Table 1), which are indeed more close to that obtained by surface tension method. For C_{12}-2-C_{12} 2Br, the value obtained by procedure 1 is very close to the *cmc* measured by surface tension technique, indicating the existence of the relatively suitable microenvironment for pyrene solubilization. This is perhaps due to its cylindrical molecular geometry benefitting to aggregation. The present result also indicates that the added pyrene only with very small quantity should have no disturbance for the surfactant aggregation. The I_1/I_3 values at the nearly horizontal part at high concentration decreases with the addition of NaBr (Table 2).

Table 2 The values of I_1/I_3 for C_{12}-*s*-C_{12} 2Br solutions in the absence and the presence of NaBr

C_{NaBr}/mmolL^{-1}	0	1	10
C_{12}-2-C_{12} 2Br	1.29	1.25	0.95
C_{12}-4-C_{12} 2Br	1.44	1.43	1.42
C_{12}-6-C_{12} 2Br	1.47	1.46	1.45
C_{12}-12-C_{12} 2Br	1.42	1.41	1.35

This agrees with the more tightly packing of surfactant molecules in the aggregates owing to the screening effect of the added salt on the ionic head groups of surfactants.

Strong adsorption induced by NaBr

The concentration (C_{20}) required to reduce 20-mN m^{-1} surface tension of water characterizes the efficiency in surface tension reduction [1]. In order to compare the NaBr effect, the ratio of C_{20} to C_{20}^0, where C_{20}^0 represents that in the case without NaBr, is plotted as a function of the NaBr concentration C_{NaBr} as shown in Fig. 4. From the insert where the local parts over the range of low NaBr concentration are enlarged, one can clearly observe considerable reduction in the C_{20} of C_{12}-s-C_{12} 2Br at only 0.1 mmol L^{-1} salt, while that of C_{12}TABr is almost unchanged even at 1 mmol L^{-1} NaBr. With increasing C_{NaBr} up to 10 mmol L^{-1}, the C_{20} of C_{12}-s-C_{12} 2Br drops to a quite small value (see Table 1) and the ratio C_{20}/C_{20}^0 has been almost close to that at 100 mmol L^{-1} NaBr. For C_{12}TABr, however, the effect of 10 mmol L^{-1} NaBr is only moderate and its ratio C_{20}/C_{20}^0 continuously decreases until a small value at 100 mmol L^{-1} NaBr. These indicate that NaBr effectively enhances the efficiency of C_{12}-s-C_{12} 2Br in surface tension reduction. As mentioned in the "Introduction," even at s=6, the stretched length (d_s) of the spacer is still somewhat smaller than the electrostatic equilibrium distance between the quaternary ammonium heads. The concentrated charges in the "head region" of C_{12}-s-C_{12} 2Br at $s \leq 6$ are thus quite sensitive to NaBr. For C_{12}-12-C_{12} 2Br, Alami et al. [11] suggested that the long spacer bends toward the alkyl tails. This leads to the high densities not only in the charge of the "head region" but also in the alkyl tails, and thus the reduction in C_{20} is again sensitive to NaBr. The present results give out significant information that the effect of salt can be adjusted by changing the length of spacer in C_{12}-s-C_{12} 2Br, which will be also observed for the other properties as discussed below.

The minimum surface tension (γ_{cmc}) at the *cmc* is generally used to characterize the effectiveness in surface tension reduction [1]. Figure 5 shows the plots of the ratio $\gamma_{cmc}/\gamma_{cmc}^0$, where γ_{cmc}^0 represents that in the case without NaBr, as a function of C_{NaBr}. With the addition of NaBr up to 10 mmol L^{-1}, the γ_{cmc} for all gemini systems reduces. This can be interpreted by the screening of salt to the head charge, which promotes the molecules packing tightly at the air/water interface. C_{12}-2-C_{12} 2Br has the shortest spacer and its ionization degree of the micelle was found to have the smallest value in this series of surfactants [4]. This leads to the lesser net charge in its head and thus corresponds to the smallest reduction in γ_{cmc} with the addition of NaBr. This is also similar to the case of C_{12}TABr that has a comparable ionization degree of the micelle with C_{12}-2-C_{12} 2Br (0.24 for C_{12}TABr [17] and 0.22 for C_{12}-2-C_{12} 2Br [4]) and thus a relatively small reduction in γ_{cmc} with increasing C_{NaBr}. Comparatively, C_{12}-12-C_{12} 2Br exhibits a pronounced decrease in γ_{cmc}, which obviously relates to its long spacer. It was known that the long spacer is bent toward the air side [11]. However, the folding extent may

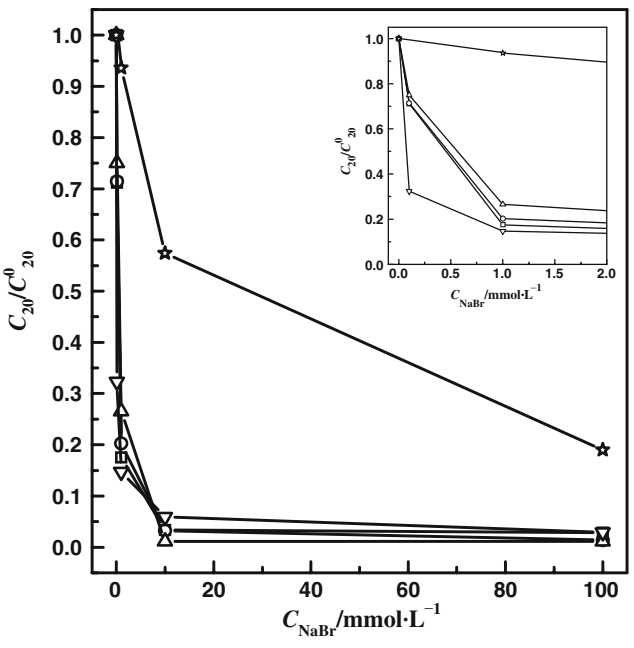

Fig. 4 Dependence of the ratio C_{20}/C_{20}^0, where C_{20}^0 represents that in the case without NaBr, of surfactant aqueous solutions on the concentration of NaBr: (*squares*) C_{12}-2-C_{12} 2Br, (*circles*) C_{12}-4-C_{12} 2Br, (*upright triangles*) C_{12}-6-C_{12} 2Br, (*inverted triangles*) C_{12}-12-C_{12} 2Br, and (*stars*) C_{12}TABr. The *insert* shows the enlarged part over the range of low NaBr concentration

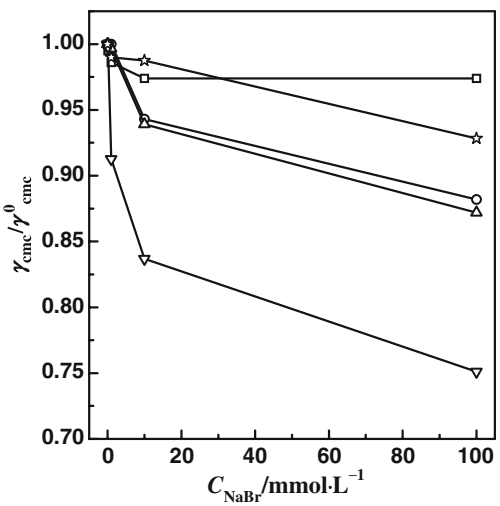

Fig. 5 Plots of the ratio $\gamma_{cmc}/\gamma_{cmc}^0$, where γ_{cmc}^0 represents that in the case without NaBr, of surfactant aqueous solutions as a function of C_{NaBr}: (*squares*) C_{12}-2-C_{12} 2Br, (*circles*) C_{12}-4-C_{12} 2Br, (*upright triangles*) C_{12}-6-C_{12} 2Br, (*inverted triangles*) C_{12}-12-C_{12} 2Br, and (*stars*) C_{12}TABr

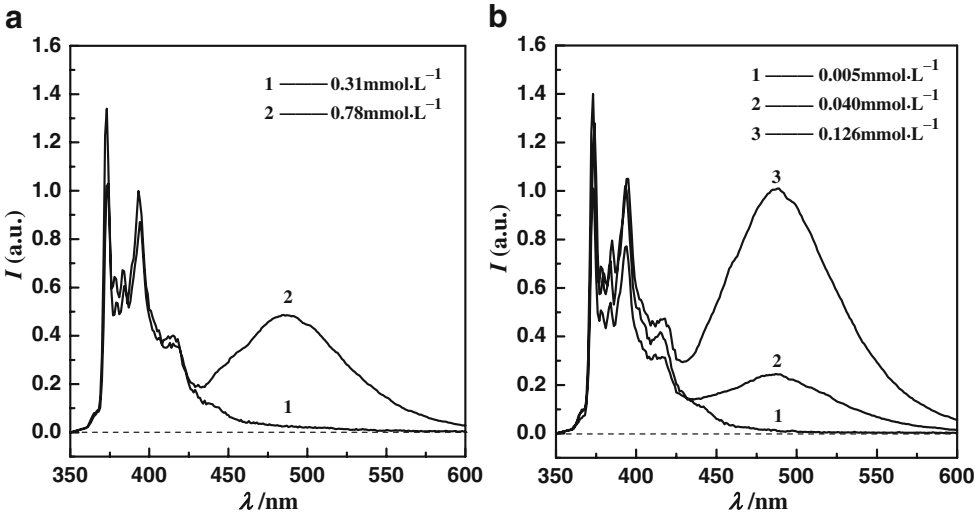

Fig. 6 Emission spectra of pyrene (5×10^{-6} mol L^{-1}) in C_{12}-4-C_{12} 2Br aqueous solutions in the presence of 1 mmol L^{-1} NaBr (**a**) and of 10 mmol L^{-1} NaBr (**b**). The *Arabic numerals* in the *graphs* represent the surfactant concentration in the bulk solution. For convenience, these designed concentrations are also marked in Fig. 1b by the same Arabic numerals

be still limited in the absence of salt. When adding NaBr, the electrostatic repulsion between the ionic head groups is reduced and the distance between the two heads within one molecule is effectively shortened. This promotes the hydrophobic interaction between the bent spacer and the alkyl tails and thus the spacer chain strongly folds [18]. As a result, C_{12}-12-C_{12} 2Br molecules are more and more tightly packed at the interface and the γ_{cmc} considerably decreases with C_{NaBr}. These results indicate that addition of NaBr enhances the effectiveness of C_{12}-*s*-C_{12} 2Br in surface tension reduction. The extent of their response to salt depends on the spacer length, which is an important character of gemini-type surfactant superior to the corresponding conventional surfactant.

Premicellization induced by NaBr

Sakai et al. [13] previously observed two break points on the γ versus log*C* curves in fatty acid *N*-methylethanolamide aqueous solution and suggested the break point at higher concentration to be the critical concentration of the normal micelle formation (*cmc*). They confirmed the existence of premicellar aggregates in the concentration region between the two break points since the emission spectrum of the probe pyrene showed a broad band at 485 nm, which is generally an index of pyrene excimer formation [12]. Similar fluorescent experiments are also carried out for the present systems. Three examples are shown in Figs. 6 and 7, respectively. For C_{12}-4-C_{12} 2Br aqueous solution at 1 mmol L^{-1} NaBr, the broad band at 485 nm is not observed before the *cmc* (as noted by Arabic numeral 1 in Fig. 6a) but appears in the region of normal micelle formation (noted by 2 in Fig. 6a, which is beyond the *cmc* as shown in Fig. 1b). At 10 mmol L^{-1} NaBr (Fig. 6b), however, a clear broad band is observed (noted by 2) at the concentration between the two break points on the surface tension curve (see Fig. 1b). For C_{12}-12-C_{12} 2Br aqueous solution at 100 mmol L^{-1} NaBr, though the surface tension rapidly drops with *C*, the broad band at 485 nm is not observed before the *cmc* (noted by 1, Fig. 7). The formation of pyrene excimer means that the probe molecules are concentrated in the local microenvironment, indicating the existence of aggregates with the core–shell structure for surfactant aqueous solution, even though this structure may be uncompleted. Therefore, the results of Fig. 6 give out the clear evidence that small aggregates exist in the solution in the concentration region between the two break points of the surface tension curve. For C_{12}TABr system (Fig. 2), one does not observe two break points on the γ versus log*C* curve even at 100 mmol L^{-1} NaBr, i.e., no premicellization occurs in C_{12}TABr system. This indicates that the addition of NaBr promotes the interaction between C_{12}-*s*-C_{12} 2Br molecules in aqueous solution. Similarly, the above results are attributed to the head

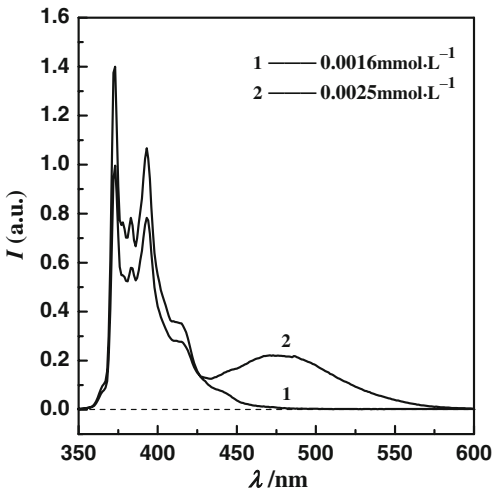

Fig. 7 Emission spectra of pyrene (5×10^{-6} mol L^{-1}) in C_{12}-12-C_{12} 2Br aqueous solutions in the presence of 100 mmol L^{-1} NaBr. The representation of the Arabic numerals is similar to Fig. 6 and is also marked in Fig. 1d

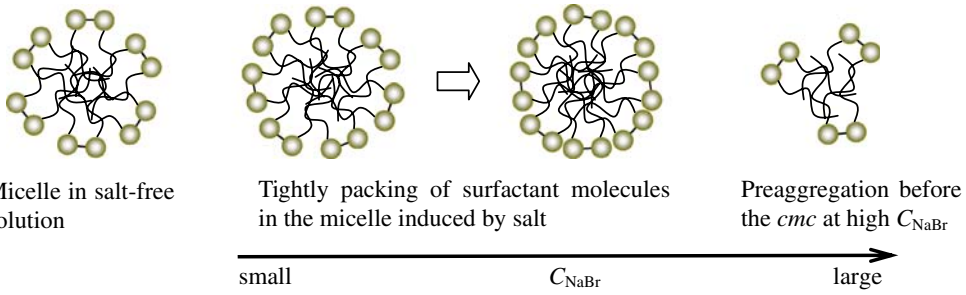

Fig. 8 A schematic representation for the effect of salt on the aggregate structure

structure of C_{12}-*s*-C_{12} 2Br different from C_{12}TABr as discussed in the above section. Thus, the addition of NaBr not only effectively reduces the electrostatic repulsion between the ionic heads but also greatly enhances the hydrophobic interaction between the alkyl tails, resulting in strong aggregation of C_{12}-*s*-C_{12} 2Br in aqueous solution.

Premicellar aggregation has occurred in the solutions of some cationic gemini surfactants that are sufficiently hydrophobic, for example, for C_{12}-*s*-C_{12} 2Br dimers with $s>12$ and for C_m-8-C_m 2Br dimers with $m\geq14$, respectively [19]. When *p*-xylylene or monohydroxypropyl was used as the spacer, premicellar association was present for C_m-xylyl-C_m 2Br or C_m-hop-C_m 2Br dimers with $m\geq 14$ [19, 20]. Compared with these dimers, it would be impossible for the examined gemini surfactants except C_{12}-12-C_{12} 2Br to produce premicellar aggregation owing to relatively low hydrophobicity of the surfactant molecule. The present result well indicates the strong effect of added salt on the aggregation of C_{12}-*s*-C_{12} 2Br. Combining the results of the micelle micropolarity characterized by I_1/I_3 (see above), Fig. 8 gives out a schematic representation for the effect of salt on the aggregate structure, in which with increasing NaBr concentration the surfactant molecules pack more tightly in the micelle and even produce the premicellization at high NaBr concentration.

It is notable why the premicellization does not occur in C_{12}-12-C_{12} 2Br even at 100 mmol L^{-1} NaBr. This is perhaps due to its quite strong trend for adsorption as seen in Table 1, where the C_{20} of C_{12}-12-C_{12} 2Br (0.034) is one order of magnitude smaller than that of the other geminis. This indicates that C_{12}-12-C_{12} 2Br prefers to adsorb at the interface in the presence of NaBr rather than to associate in the solution.

Very low *cmc* in the presence of NaBr

The critical micelle concentration (*cmc*) is generally used to characterize the ability of micelle formation [1]. Figure 9 shows the plots of the ratio cmc/cmc^0, where cmc^0 represents that in the case without NaBr, as a function of C_{NaBr}. One can find that the *cmc* of C_{12}-*s*-C_{12} 2Br is also very sensitive to salt. Even at 0.1 mmol L^{-1} NaBr, their *cmc*s have exhibited clear decrease compared with that in the salt-free system. Similar to C_{20}, the *cmc* at 10 mmol L^{-1} NaBr reduces to low value close to that at 100 mmol L^{-1} NaBr (see Table 1). Comparatively, the reduction in the *cmc* of C_{12}TABr is much smaller than that of C_{12}-*s*-C_{12} 2Br even at 100 mmol L^{-1} NaBr.

Conclusion

The present results show that the self-assembly of C_{12}-*s*-C_{12} 2Br is strongly promoted by the addition of NaBr, which is attributed to the unique molecular structure of gemini surfactant. Owing to the flexible polymethylene chain as the spacer linking the two quaternary ammonium heads, the charges of the two quaternary ammonium head groups are concentrated by a short spacer or a long one but folding toward the alkyl tails, resulting in the high sensitivity of

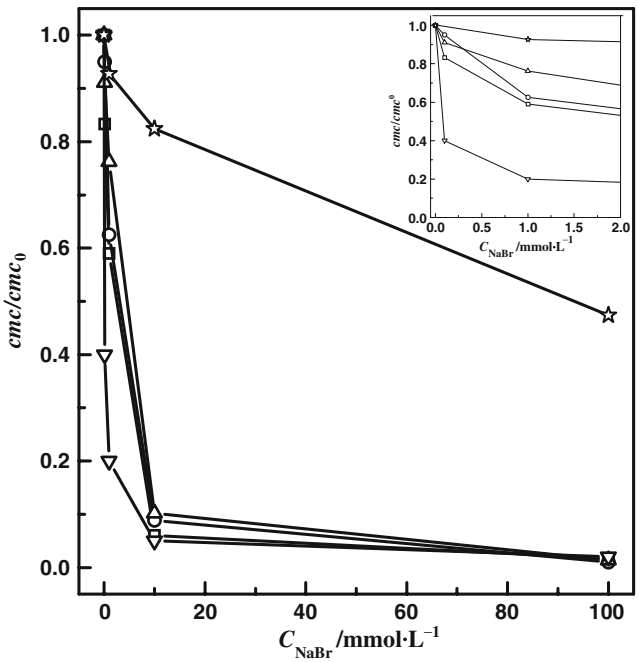

Fig. 9 Plots of the ratio cmc/cmc^0, where cmc^0 represents that in the case without NaBr, as a function of C_{NaBr}: (*squares*) C_{12}-2-C_{12} 2Br, (*circles*) C_{12}-4-C_{12} 2Br, (*upright triangles*) C_{12}-6-C_{12} 2Br, (*inverted triangles*) C_{12}-12-C_{12} 2Br, and (*stars*) C_{12}TABr. The *insert* shows the enlarged part over the range of low NaBr concentration

their ionic head groups to salt. So high sensitivity of gemini-type surfactant to salt will be useful for promoting the self-assembly of the mixed surfactant systems containing ionic gemini component. Moreover, it is also of significance that the high sensitivity to salt can be adjusted by changing the spacer length within the gemini molecule, which will perhaps provide us a simple and convenient approach to control the interaction between surfactant molecules.

Acknowledgment Support from the National Natural Science Foundation of China (20673021) and the Professional Foundation of FZU (XRC-0639, 2008-XY-5) is gratefully acknowledged.

References

1. Rosen MJ (1988) Surfactants and interfacial phenomena, 2nd edn. Wiley, New York
2. Menger FM, Littau CA (1993) J Am Chem Soc 113:1451–1452
3. Menger FM, Littau CA (1993) J Am Chem Soc 113:10083–10090
4. Zana R, Benrraou M, Rueff R (1991) Langmuir 7:1072–1075
5. De S, Aswal VK, Goyal PS, Bhattacharya S (1996) J Phys Chem 100:11664–11671
6. Grosmaire L, Chorro M, Chorro C, Partyka S, Zana R (2002) J Colloid Interface Sci 246:175–181
7. Zana R (2002) J Colloid Interface Sci 248:203–220
8. Danino D, Talmon Y, Zana R (1995) Langmuir 11:1448–1456
9. Zana R (2002) Adv Colloid Interface Sci 97:203–253 and references therein
10. Zana R, Xia JD (2004) Gemini surfactants. Marcel Dekker, New York
11. Alami E, Beinert G, Marie P, Zana R (1993) Langmuir 9:1465–1467
12. Valeur B (2001) Molecular fluorescence, principles and applications. New York, Wiley
13. Sakai T, Kaneko Y, Tsujii K (2006) Langmuir 22:2039–2044
14. Frindi M, Michels B, Zana R (1992) J Phys Chem 96:8137–8141
15. Zana R, Lévy H, Kwetkat K (1998) J Colloid Interface Sci 197:370–376
16. Anthony O, Zana R (1994) Macromolecules 27:3885–3891
17. Zana R (1980) J Colloid Interface Sci 78:330–337
18. You Y, Jiang R, Ling TT, Zhao JX (2009) Chin J Chem 27:1–10 (in English)
19. Zana R (2002) J Colloid Interface Sci 246:182–190
20. Song LD, Rosen MJ (1996) Langmuir 12:1149–1153